Phase-sensitive optical coherence tomography imaging of the tissue motion within the organ of Corti at a subnanometer scale: a preliminary study

Ruikang K. Wang
Oregon Health & Science University
Department of Biomedical Engineering
and
Department of Anesthesiology and Peri-Operative Medicine
CH13B
3303 Southwest Bond Avenue
Portland, Oregon 97239

Alfred L. Nuttall
Oregon Health & Science University
Department of Biomedical Engineering
CH13B
3303 Southwest Bond Avenue
Portland, Oregon 97239
and
Oregon Health & Science University
Oregon Hearing Research Center
NRC04
3181 Southwest Sam Jackson Park Road
Portland, Oregon 97239

Abstract. Hearing loss can mean severe impairment to the quality of life. However, the biomechanical mechanisms of how the hearing organ, i.e., the organ of Corti (OC), responds to sound are still elusive, largely because there is currently no means available to image the 3-D motion characteristics of the OC. We present a novel use of the phase-sensitive spectral domain optical coherence tomography (PSOCT) to characterize the motion of cellular compartments within the OC at a subnanometer scale. The PSOCT system operates at 1310 nm with a spatial resolution of ~16 μm and an imaging speed of 47,000 *A*-lines/s. The phase changes of the spectral interferograms induced by the localized tissue motion are used to quantify the vibration magnitude. Fourier transform analysis of the phase changes improves the system sensitivity to sense minute vibrations smaller than 1 nm. We demonstrate that the PSOCT system is feasible to image the meaningful vibration of cellular compartments within the OC with an unprecedented sensitivity down to ~0.5 Å. [DOI: 10.1117/1.3486543]

Keywords: phase-sensitive measurement; spectral domain optical coherence tomography; tissue nanomotion; organ of Corti; hearing.

Paper 10140RRR received Mar. 19, 2010; revised manuscript received Jul. 5, 2010; accepted for publication Jul. 23, 2010; published online Sep. 10, 2010.

1 Introduction

The mammalian cochlea is a remarkably sensitive hearing organ that can detect displacements at angstrom level (e.g., Ref. 1). When the ear drum receives a sound pressure wave, it passes the sound to the middle ear, causing vibration of the ossicular chain that travels, via the oval window, to the fluid-filled cochlea, where fluid waves in the perilymph are generated. The fluid pressure of the perilymph causes a wavelike displacement of the organ of Corti (OC) and its basilar membrane (BM). These displacement traveling waves of motion that propagate along the BM and OC are responsible for the acoustic frequency tuning and the extraordinary sensitivity of the hearing organ that ultimately stimulates the mechanosensory receptor cells. The formidable functions of the cochlea are realized by a so-called "cochlear amplifier," an entity whose mode of operation somehow depends on the sound-induced motile responses of specialized cells, called outer hair cells (OHCs). The cochlear amplifier must involve a complex biophysical interplay between molecular, cellular, and hydrodynamic processes. In spite of remarkably rapid progress in hearing research, the amplification process is still not understood.

There is significant controversy in the field of cochlear mechanical measurements over the spatial motion pattern of the BM and of the cellular components of the OC in response to sound, particularly at low levels. The cochlear amplifier has been proposed as the mechanism responsible for increasing BM motion when low-level sounds stimulate the ear. The hypothesis is that the cochlear amplifier uses biologically produced force or dynamic system stiffness changes at acoustic frequencies. The most popular and widely accepted model for the cochlear amplifier posits force generation from voltage-sensitive (electromotile) proteins inserted[2] in the basolateral wall of the OHCs, but an alternative possibility is force production from the stereocilia located at the apical end of each outer hair cell.[3,4] In the mammalian cochlea, the hypothesized positive feedback of force from OHCs to BM motion has been of great interest for more than 20 yr. Kim et al.[5] were the first to suggest a local active process. This was followed 5 yr later by the discovery of OHC electromotility.[6] OHCs possess a piezoelectric-like force production system, as well as a calcium-binding force production system. Just how the OC amplification and sharp tuning are achieved is not yet known. This is largely because there is currently no appropriate means available to access this delicate organ for accurate measurements of magnitude and phase of its cellular elements' motion. Therefore, an imaging means capable of characterizing the 3-D, minute motion of the hearing organ when stimulated by sound would represent a significant advance in hearing research.

Address all the correspondence to: Ruikang K. Wang, Oregon Health & Science University, Department of Biomedical Engineering, CH13B, 3303 Southwest Bond Avenue, Portland, Oregon 97239. Tel: 503-418-9317; Fax: 503-418-9317. E-mail: wangr@ohsu.edu

1083-3668/2010/15(5)/056005/9/$25.00 © 2010 SPIE

Laser interferometry and its variations are probably the only techniques currently available in the hearing research community to nondestructively measure the motion/displacement of the OC, usually on the BM. There are two unique problems when using optical techniques to measure inner-ear tissue vibration. First, the OC has a low level of reflectance, because the refractive index of the tissue is very close to that of inner-ear fluids surrounding the tissue. Khanna et al.[7] found BM reflectance levels at a 633-nm wavelength of approximately 3×10^{-4} to 3×10^{-5}. The second problem is the magnitude of motion of the living OC. The motion magnitudes of interest in the OC range from a fraction of a nanometer to about one micrometer. However, the most interesting biology occurs between 0.1 and 10 nm. These problems impose the requirements for the measuring techniques to be sensitive to low-level light reflectance (i.e., >100-dB sensitivity) and to the displacement at a subnanometer scale. In addition, the cochlear amplifier hypothesis demands that the measuring technique be able to image the 3-D motion of the OC with a resolution at a cellular level.

To cope with the low-level reflectance from the OC, optical interferometry often requires that reflecting beads be applied onto the surface of the BM to enhance the optical reflectance from the tissue surface, so they can be detected. Such an approach is not desirable for the living OC, because the applied beads may alter the functions of the OC. While the confocal slit-scanning interferometer system is capable of direct measurements from tissue[8] (no reflective objects, such as beads, need be placed on the tissue), its carrier-to-noise ratio (SNR) is generally so low that it limits its use to high-vibration levels (sounds above a 50-dB sound pressure level[8]). There are also some "beadless" optical measurements suggested by Gummer et al., but only from the reticular lamina (RL) surface in the apical turn.[9] The most successful development for BM motion studies without reflective beads has been laser self-mixing interferometry.[9–11] Although the results from these techniques are sometimes encouraging, these techniques for *in vivo* use are limited to the single-point measurements, thus they do not offer the motion scenario among the different cellular compartments in two and three dimensions, which is required to address the hypothesis of the cochlear amplifier.

Optical coherence tomography[12,13] (OCT), especially[14] after its advent of Fourier domain OCT (FDOCT), is a very promising and noninvasive tool capable of providing high-speed and high-sensitivity (>100-dB) 3-D imaging of biological tissues. By utilizing low-coherence interferometry, OCT performs optical ranging within a sample that enables the visualization of microstructures in biological tissue based on local optical scattering properties, with imaging resolutions approaching that for conventional histology. OCT is becoming the most successful optical technology to date in disease diagnostics. It was initially validated as an imaging technique to study healthy and diseased retinas[15,16] and then quickly evolved into a diagnostic tool for use in clinics for other organs (e.g., Refs. 17 and 18). Recently, OCT has been used for the inner-ear imaging studies in animal models, which demonstrated the OCT capability for distinguishing different structural and morphological features of the cochlea *in situ* and *ex vivo*,[19,20] as well as *in vivo*.[21] By using a time-domain OCT (TDOCT) system with its inherent low system sensitivity (<100 dB) and low imaging speed, these previous studies were only able to provide cross-sectional (2-D) images of the cochlea under study, which is not ideal for hearing research. Most recently, there were reports of using an ultrafast, spectral domain OCT system for 3-D morphological imaging of the cochlea in mice *in vivo*, with an imaging rate[22] of 2 volumes/s.

Hong and Freeman[23] were the first to use OCT to study cochlear mechanics, where they employed an extension of the OCT technique,[24] i.e., Doppler OCT (DOCT), that relied on the Doppler effect induced by tissue motion to measure tissue displacement.[25,26] However, it was quickly realized that the reported DOCT was not capable of measuring the minute tissue motion in the OC at the nanometer scale. Later, Chen et al.[27] reported a novel use of the TDOCT to measure tissue vibration of the OC, in which the low-coherence properties of the light source and a lock-in amplifier were used to realize a localized spectrum analyzer for measuring tissue vibration at a nanometer scale. Although the results were encouraging, such implementation of TDOCT faced several challenges that must be addressed to investigate the 3-D mechanical properties of the OC in response to a wide frequency and intensity range of acoustic pressures. These challenges were first, the system provided only a single-point measurement at any one time, which limits the quality of the measurement procedure for the many points of interest within the OC. Second, to improve the system SNR and give absolute calibration, a vibrating piezo mirror with a known frequency of vibration had to be used in the reference arm, so the system could be tuned, usually manually, to the most sensitive region of a cosine function. This tuning to the sensitive region was often difficult to achieve in practice. These problems make the current TDOCT system extremely difficult, if not impossible, to apply and address the critical issues that require us to measure the motion of the OC in two and three dimensions.

To meet the aforementioned challenges of using the TDOCT system, in this paper, we report a novel use of phase-sensitive OCT (PSOCT) to measure the nanomotions of the OC. The method is based on spectral domain implementation of the OCT system recently developed in the OCT research community[14,28] and analyzes the phase information contained in the OCT signals. Followed by a Fourier transform (FT) analysis of the measured phase changes in the spectral interferograms induced by the nanomotion of the OC, we demonstrate that PSOCT is able to characterize and image the vibration of cellular compartments in the OC with an unprecedented sensitivity down to ~0.5 Å.

Note that the concept of using the phase information of the OCT signals has been explored previously to detect the sample displacement at a sensitivity of tens of picometers.[29–33] These prior methods are mostly based on common-path optical coherence tomography, so the system is stable enough to measure the slow dynamic changes of cells.[29–33] Recent development has seen the use of PSOCT, still based on the common-path configuration, to detect the photothermal effect of nanoparticles embedded within the gel phantoms.[34,35] However, we realized that the common-path configuration does not offer flexibility for the user, since the reference reflector must always be close to the sample structure. This was particularly problematic for the current study of imaging the responses of

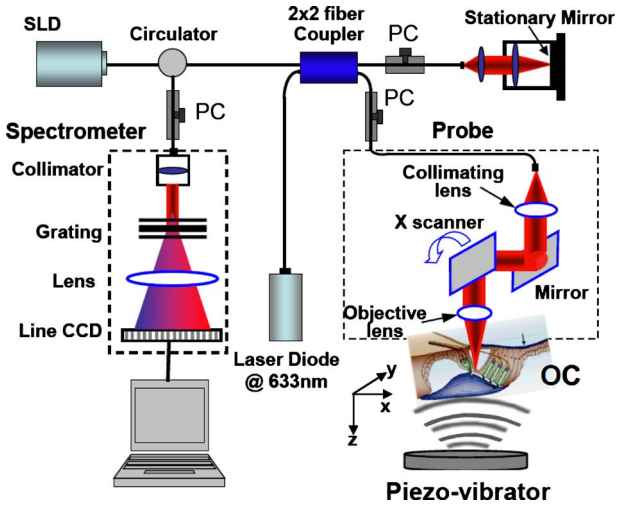

Fig. 1 Schematic of the PSOCT system used in this study to measure the nanomotion within OC, where PC represents the polarization controller, and CCD, the charged coupled device. A laser diode emitting light at 633 nm was used for aiming purposes during imaging.

the OC to the sound stimulation. In this paper, we apply PSOCT by using conventional system setup to achieve our goal of measuring tissue motion in the OC. Because we were interested in the frequency response of the OC at the base turn, whose range is between 12 and 20 KHz, the system noise and slow sample motion would have a minimal effect on our ability to measure the tissue vibration of the OC.

2 Methods and Material

2.1 *System Setup*

The PSOCT system setup we used in this study is shown schematically in Fig. 1, similar to our previous studies.[36,37] The system employed conventional spectral domain OCT (SDOCT) to achieve ultra-high-sensitive measurement of the phase changes within the spectral interferograms induced by the nanomotion of the cellular components within the OC. We used a superluminecent diode (SLD, Denselight Ltd., Singapore) with a central wavelength of 1310 nm and a spectral bandwidth of 56 nm as the light source, which provided an axial imaging resolution of ~13 μm in air (~9 μm within the OC, assuming the refractive index is 1.42). We coupled the light from the SLD into a fiber-based Michelson interferometer, via an optical circulator. In the reference arm, we delivered the light onto a stationary mirror. In the sample arm, we focused the light into a sample via an objective lens.

With a 50-mm-focal-length objective lens in the sample arm, the size of the focus spot on the sample was ~16 μm, i.e., the lateral resolution of the system was ~16 μm. The zero-delay line of the system was set at ~0.5 mm above the focus spot of the sample beam, at which position we carefully placed the OC. A 2×2 optical fiber coupler recombined the light backscattered from the sample and reflected from the reference mirror. Then, we routed this combined beam to a home-built, high-speed spectrometer via the optical circulator. The spectrometer consisted of a 30-mm-focal-length collimator, a 1200-lines/mm transmitting grating, an achromatic lens with a 100-mm focal length, and a 14-bit, 1024-pixels InGaAs line scan camera (Goodrich Ltd., United States). This spectrometer setup had a designed spectral resolution of 0.141 nm, which gave a measured imaging depth of ~3.0 mm on the each side of the zero-delay line. The line-scan rate of the camera was ~47 KHz. With this line-scan rate, we measured the SNR at 0.5 mm axial depth position at ~100 dB and the phase noise at ~3.0 mrad.

In the sample arm, the probing beam can be scanned by an x-y galvoscanner in a raster fashion. In most of the experiments we report in this paper, the galvoscanner was disabled, so we acquired the time-varying spectral interferograms (M-mode scanning) to perform the quantitative analysis of the nanometer-scale vibration within sample (see in the following). In other experiments, to provide the vibration distribution over cross section of the sample (B scan), we performed M-B mode scanning.

2.2 *Phase-Sensitive Measurement of Nanovibration Along the Axial Depth in Parallel*

In the SDOCT, as shown in Fig. 1, it is not necessary to scan the reference mirror to perform the depth scan. In other words, the reference mirror is stationary during imaging, as opposed to moving, as it is in TDOCT. However, the detection system is an optical spectrometer, which acquires the interference spectrum formed between the reference light and the backscattered light from within a tissue sample. The detected intensity spectrum is then Fourier transformed into the distance (i.e., time domain) to reconstruct the depth-resolved sample optical microstructures. Thus, SDOCT can measure the vibration at every position along the entire imaging depth in parallel. This is a tremendous advantage, because it solves[27] the problem of single-point measurement faced by the previous TDOCT, making rapid imaging of the OC possible.

The basic concept of using PSOCT to measure the vibration has been discussed elsewhere.[32,34,35] Assume the detected interference spectrum is $I(k)=2|E_R E_S|\cos(2kz+\varphi)$, where $k=2\pi/\lambda$, z is the depth coordinate within the sample, and φ is a random phase due to the optical system noise. The depth-resolved structural signal, i.e., an OCT A-scan, is obtained from a FT of $I(k)$ over k into the time-domain interference signal $I(z)$ (note that $z=ct$, where c is the speed of light):

$$I(z)=\mathrm{FT}[I(k)]=M(z)\exp[i\Phi(z)], \tag{1}$$

where $M(z)$ is the magnitude used to reconstruct the conventional OCT structural images of the sample, and $\Phi(z)$ is a random phase caused by the microstructures located at the depth z, as well as φ. Here, our imaging target is the OC. When the OC receives sound stimulation, its constituent cellular compartments would respond with different degrees of vibration magnitude relative to the stimulation sound, which ultimately stimulate the mechanosensory receptors. In this case, the vibration of the cellular compartments in the OC will cause optical path length changes of light that are backscattered by the scatters located at position z within the OC over time t, which subsequently induces phase changes in the OCT signals. Thus, assuming the sound stimulation is of a single frequency, the phase term in Eq. (1) becomes

$$\Phi(z,t) = \frac{4\pi}{\lambda} A \sin(2\pi f_0 t) + \varphi, \tag{2}$$

where A and f_0 are the magnitude and frequency, respectively, of a sinusoidal vibration source. A differentiation operation to Eq. (2) can be performed to eliminate the phase term φ:

$$\Delta\Phi(z,t) = \frac{8\pi^2}{\lambda} A f_0 \cos(2\pi f_0 t)\Delta t + \xi(t). \tag{3}$$

Here, $\xi(t)$ is a phase noise caused by the system noises, including photon shot noise, thermal noise, and electronic noise, and Δt is reciprocal of the sampling frequency. Thus, from the measurement of the phase difference in the OCT signals, the vibration information can be retrieved, as long as the noise term $\xi(t)$ is small compared to $\Delta\Phi(z)$. This concept is similar to the phase-resolved Doppler OCT (PRDOCT) method that was developed to successfully measure fluid flow, e.g., blood flow, within a tissue sample.[24,38] Following the PRDOCT approach, the phase difference between adjacent A scans, j and $j-1$, can be calculated as:

$$\Delta\Phi(z,t) = \arctan\{\mathrm{Im}[I(z,t_j)I^*(z,t_{j-1})] / \mathrm{Re}[I(z,t_j)I^*(z,t_{j-1})]\}, \tag{4}$$

where * denotes the complex conjugate. However, for our purpose of measuring the vibration of the OC in response to sound, the magnitude of vibration is normally at the subnanometer scale. For example, if the tissue vibrates at 0.2 nm, the maximum phase change $\Delta\Phi(z)$ will be as small as ~2 mrad, which is below the noise floor $\xi(t)$ of an OCT system (~3 mrad for the system setup shown in Fig. 1).

To overcome this limitation, we used the Fourier frequency analysis approach for Eqs. (3) and (4) to improve the system sensitivity further to measure phase changes. This concept is similar to the spectrum analysis in the signal-processing discipline. FT of Eq. (3) gives

$$p(z,f) = \mathrm{FT}[\Delta\Phi(z,t)] = \frac{(2\pi)^3}{\lambda} A f_0 \Delta t[\delta(f-f_0) + \delta(f+f_0)], \tag{5}$$

and the FT of the measured phase differences, i.e., Eq. (5), can be taken as

$$p(z,f) = \mathrm{FT}[\Delta\Phi(z,t)] = |p(f)|\exp[i\theta(f)]. \tag{6}$$

Here, f is the frequency variable that is of interest in the OC, and $|p(f)|$ and $\theta(f)$ are the magnitude and phase of the vibrating signal at frequency f. Thus, it is trivial that the magnitude of the vibration source at f_0 can be expressed as

$$A = \frac{|p(f_0)|\lambda_0}{(2\pi)^3 n f_0 \Delta t}. \tag{7}$$

Here, the refractive index of the sample n is taken into account in the formulation. It is known that the FT is essentially a coherent summation operation. Thus, the FT is able to "amplify" the signal of interest for detection, while it does not have an effect on the Gaussian noise (statistically). For the system we used in this study, it is reasonable that the system-phase noise is assumed to be the Gaussian noise. Therefore, the FT analysis of the measured phase changes would enhance the SNR for the signal of interest, which is essential for measuring the vibrations of the cellular compartments in the OC with a magnitude normally at a subnanometer scale.

2.3 *OC Preparation*

We used healthy guinea pigs in this study. The experimental protocol was in compliance with federal guidelines for care and handling of small rodents and approved by the Institutional Animal Care and Use Committee of Oregon Health & Science University.

Because of the delicate surgical procedures involved with the animals and for our current system to access the OC, it is currently not yet possible for us to record from live animals. Thus, we prepared the OC tissues immediately after we sacrificed the animal and brought the tissues under the PSOCT system for measurement. The preparation consisted of, first, exsanguinating the guinea pig under deep anesthesia and perfusing the vascular system with buffered saline. This procedure removed blood cells that could contaminate the cochlea following dissection. We then removed the bulla, and we opened the cochlea widely at the basal turn. We placed a small coverslip onto the cochlea to provide a flat optical field.

To introduce vibration to the OC, we used a calibrated piezostack controlled by a precision signal generator. We then mounted this prepared sample onto the piezostack using tissue cement. By securing the cochlea to the piezostack, we induced the OC to vibrate at different levels by mechanical vibration of the piezostack (see Fig. 1). We placed a moist cotton sponge around the sample to prevent it from dehydrating. This method of inducing vibration is "artificial" and simply serves to test the PSOCT system on actual cochlear tissue that is vibrating at a calibrated amount. As we describe in the following, the vibration method induced interesting differential vibration in the OC, compared to bone or the coverslip. We did not attempt to interpret these unique vibrations induced in the dead cochlea by whole bulla vibration.

3 Results and Discussion

In the preliminary studies, to validate the proposed method using the PSOCT to measure the subnanometer tissue motion in the OC, we performed a series of experiments using the PSOCT system described in Fig. 1. We first tested the method by using a vibrating piezostack as the sample. The piezostack was driven by a sinusoidal signal generated by a signal generator. We used the PSOCT system to measure the optical signals reflecting back from the surface of the piezostack for a time duration of 50 ms (i.e., M-mode scanning), and then we employed the method described in Sec. 2.2 to characterize the known vibration source. To simulate the weak back-scattering light intensity from a biological tissue, e.g., the OC, we attenuated the light impinging onto the sample by 60 dB by placing a 3-optical density neutral density filter into the path of the sample beam.

In the experiments, we measured the piezostack first without applying the vibration to it, and then with the application of vibration at an oscillating frequency of 17 KHz at magnitudes of 0.2 and 2 nm, respectively, comparable to the motion characteristics of the OC. Figure 2 shows the results. The

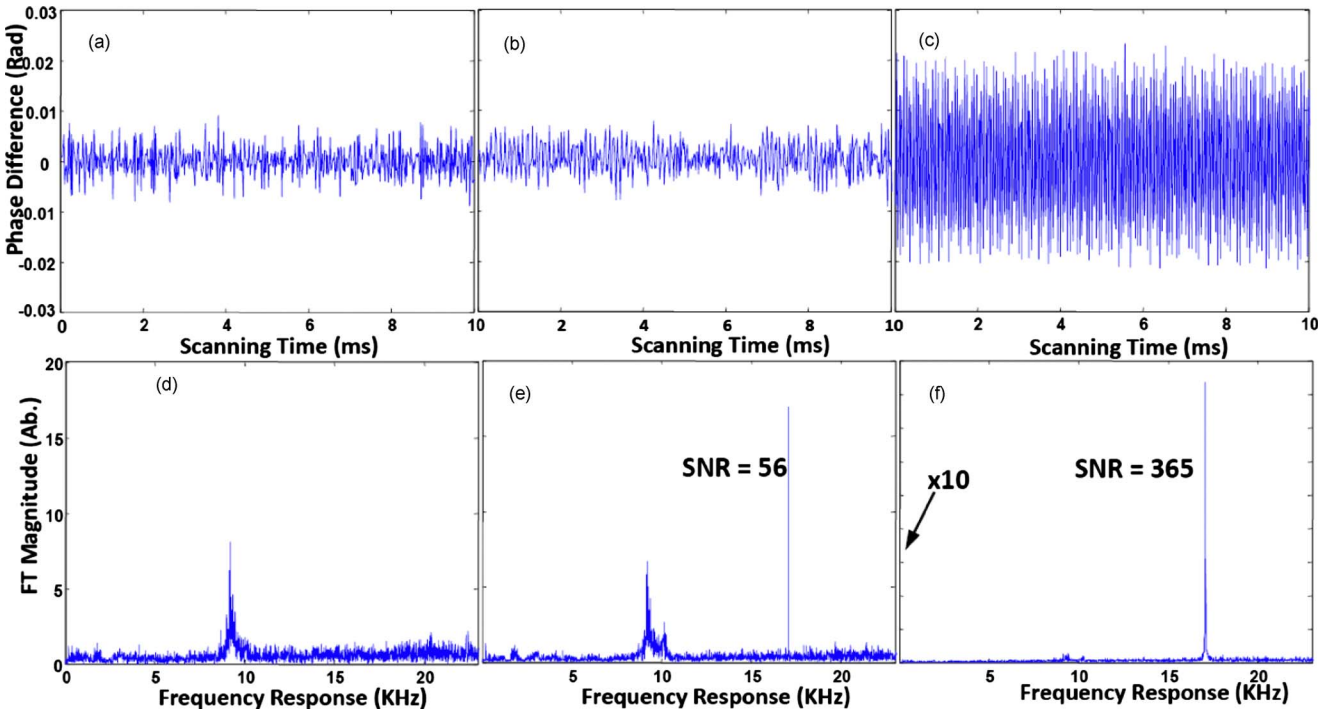

Fig. 2 Phase-sensitive measurements from a piezostack vibrating at 17 KHz: (A), (B), and (C) phase changes due to the varying optical path length induced by the piezo at a vibrating magnitude of 0 (static), 0.2, and 2 nm, respectively, and (D), (E), and (F) the corresponding frequency spectra of the phase changes in the OCT signals.

phase difference of the OCT signals from a static piezostack [Fig. 2(a)] represents the phase noise of the system that measures at root mean square (rms)=3 mrad, typical of a SDOCT system of 100-dB SNR. The FT of Fig. 2(a) shows no useful signal, as expected [see Fig. 2(d)]. Note that the frequency at ~10 KHz is an artifact due to the jitter noise from the scanning mirror that steers the light onto the sample. This can be eliminated by careful system design and the proper choice of scanners that are of high stability and reliability. For example, one can design an optimized driving circuit to drive the galvoscanner that suppresses the jitter noise at ~10 kHz. At the vibration amplitude of 0.2 nm, the phase differences of OCT signals still looked like a noise [Fig. 2(b)]. However, in the Fourier domain, the applied 17-KHz vibration was clearly contrasted with a measured SNR=~56 [Fig. 2(e)], demonstrating high sensitivity of the proposed PSOCT system. Last, with a vibrating amplitude of 2 nm, roughly at the noise level of a TDOCT system of 80-dB sensitivity, the SNR of the applied 17 KHZ vibrating signal was ~365 using our proposed method.

To test the accuracy of measured magnitude using PSOCT, we applied varying levels of vibration amplitude to the piezostack. The results are shown in Fig. 3, along with the measurements obtained independently from a standard laser vibrometer for comparison. The correlation between the measurements from PSOCT and the laser vibrometer was excellent. Note that the reliable measurement of minimal vibrating magnitude for PSOCT was ~0.05 nm, where the noise level was at ~0.03 nm, which was not achievable by the laser vibrometer or by our previous TDOCT system.[27] These measurements demonstrate the accuracy of the proposed method to measure the vibration at a subnanometer scale.

Next, we tested the proposed PSOCT system on the prepared OC from guinea pigs (see Sec. 2.3). We chose the vibration frequencies >10 kHz in the experiment, because they were meaningful to the response characteristics of the OC at the position near the cochlear basal turn. Figure 4 shows the results from one cochlea that we vibrated at 17 KHz with a magnitude of 0.2 nm. The top left corner of Fig. 4 shows a typical cross-sectional image of the OC our system obtained operating at the imaging mode, where the important physiological features of the OC are clearly demarcated, including

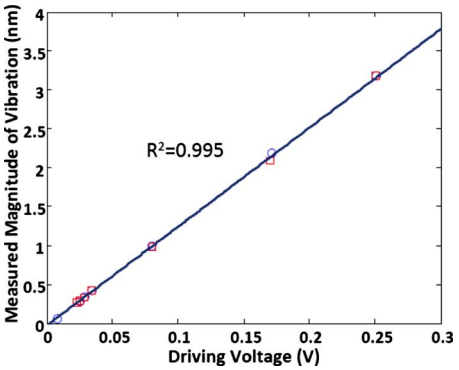

Fig. 3 Measured magnitude of vibration of a piezostack at 17 KHz by applying varying driven voltages obtained from PSOCT system (circles) and a standard laser vibrometer (squares), respectively. The lines represent the least-squares fitted curves of the corresponding measured data.

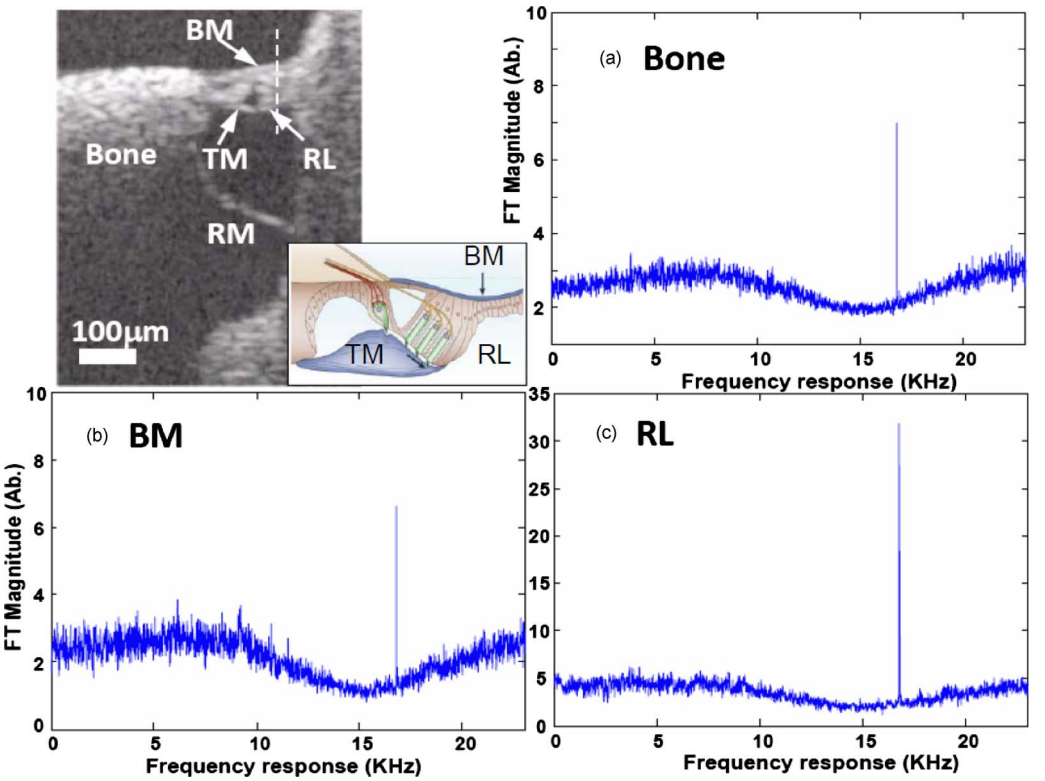

Fig. 4 PSOCT measures the frequency response from an OC vibrating at 17 KHz with magnitude of 0.2 nm, obtained from (A) bone, (B) basilar membrane, and (C) reticular lamina, respectively. The top left corner shows a typical cross sectional OCT image obtained from the PSOCT system, along with a histological drawing of the organ for comparison.

BM, RL, tectorial membrane (TM), and Reissner's membrane (RM). In addition, the region of hair cells is also visible in the OCT images. We present a histological drawing of the OC alongside for comparison, demonstrating the feasibility of the proposed system in imaging the cellular morphology of the OC. Figures 4(a)–4(c) show, respectively, the proposed PSOCT system measures of the frequency responses at different positions, where we can see that the vibration magnitude of the BM is comparable to that of the bone; however, the vibration of RL is ~8 times higher than those of the bone and BM. This is consistent with the mass and elastic properties of the OC, where the cellular structure may vibrate differently than the BM.

To demonstrate the capability of the proposed PSOCT to measure the entire depth of the OC in parallel, we analyzed the acquired data set to quantify magnitudes of vibration within the OC at the position marked in Fig. 4 (dashed line), as well as in the bone. The results are shown in Fig. 5. In the experiments, we purposely secured a coverslip on the top of the cochlea but within the imaging range of the system. We also analyzed the signals acquired from the coverslip to obtain its vibration magnitude. The vibration at the BM is first comparable to that of the coverslip, and then becomes gradually amplified when it gets farther into the depth and reaches a maximum at the RM [Fig. 5(a)]. There are no significant measurable changes along the depth in the bone [Fig. 5(c)], which vibrates at a strength approximately equal to the coverslip, demonstrating the feasibility of PSOCT to measure the meaningful frequency responses within the OC in parallel. With reference to the coverslip, the system detected a phase difference between the BM and the RL [Fig. 5(b)], while there is no phase difference seen along the depth of bone, indicating that the proposed system is also capable of measuring the phase lags that likely occur within the OC when it senses the acoustic sound pressure.

Finally, we demonstrated the capability of the proposed PSOCT to obtain the vibrating map over the entire cross section of the imaged OC. In this experiment, we enabled the x scanner in the sample arm (Fig. 1), and we used it to step the probe beam across the OC, so we were able to acquire the data set representing a cross section (i.e., M-B mode scanning). Within each step, the data acquisition time (M-mode scan) was 50 ms. There were 64 steps across the OC, requiring ~3 s to acquire the data set. We then employed the proposed data-analyzing approach to quantify the vibrating characteristics of the OC. The results are shown in Fig. 6 for two frequencies applied: 14 [Fig. 6(b)] and 20 KHZ [Fig. 6(c)], respectively. For 14 KHz, the magnitude of source vibration was 0.4 nm, while for 20 KHz, it was 0.1 nm. The results demonstrate the feasibility of PSOCT to measure the vibration characteristics of cellular tissue elements within the OC. As mentioned, we did not attempt to interpret these images, as the OC was more than 1 h postmortem, and the vibration energy was delivered as a vibration of the whole cochlea. Nevertheless, these pseudocolor intensity maps of vibration show a complexity of motion that is quite striking. They are reminiscent of the complex motion observed in phase-

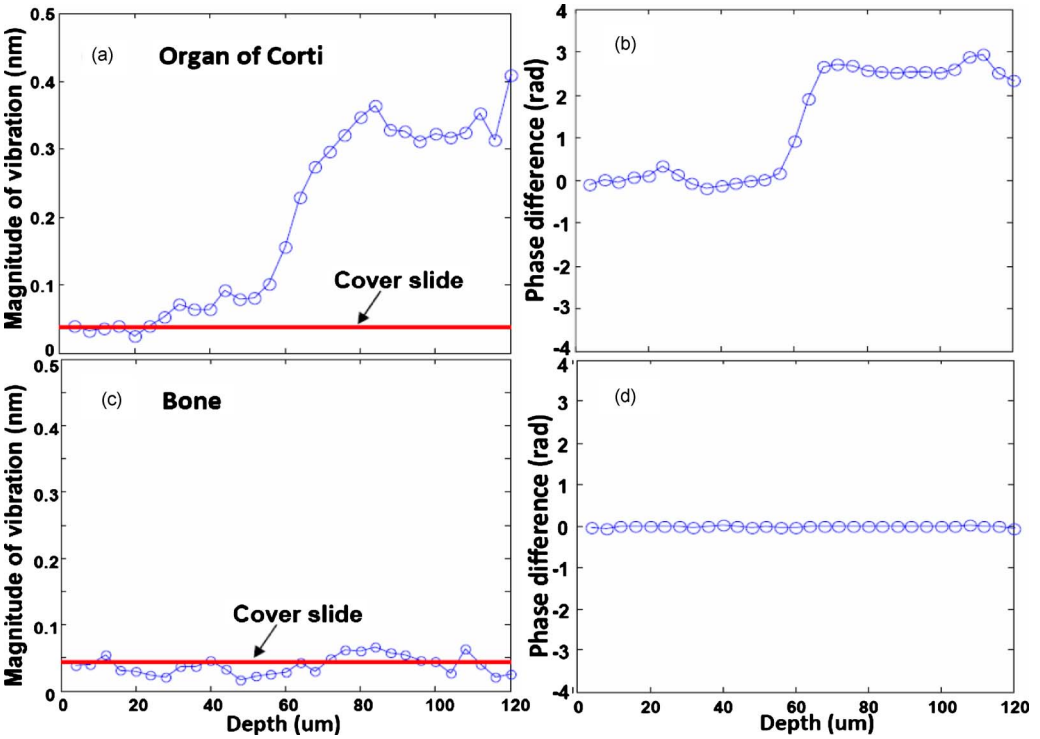

Fig. 5 Capability of PSOCT to measure the motion of the OC along the depth in parallel. The vibrating magnitudes along a depth of (A) the OC, and (C) the bone, respectively, are quantified by the PSOCT method. (B) and (D) are the corresponding phase differences of vibration with reference to the coverslip. The red line shows the measured level of vibrating magnitude from the coverslip. (Color online only.)

synchronized confocal image maps of the apical OC motion with acoustic stimulation.[39] Note here that the BM shows the greatest amount of motion consistent with the center of the membrane having a maximum and perhaps with a resonance related to the tonotopic spatial location. In Fig. 6(c), another location of maximum motion appears in the area of the inner hair cells. This brings to mind the rocking of the RL about the head plates of the pillar cells proposed by Lukashkin and Russell.[40] However, this is just conjecture at the time of these preliminary studies, and these experiments simply emphasize that the PSOCT is feasible to provide the type of spatial vibration measurement required for the next generation of cochlear mechanics study.

Currently, there are no imaging modalities other than the proposed PSOCT that can provide such highly sensitive imaging of subnanometer-scale motion of the cellular compartments within the OC. The ability of PSOCT to visualize the complex motion pattern of the entire hearing organ in response to sound stimulation could change/revolutionize our current understanding of cochlear biomechanics. However,

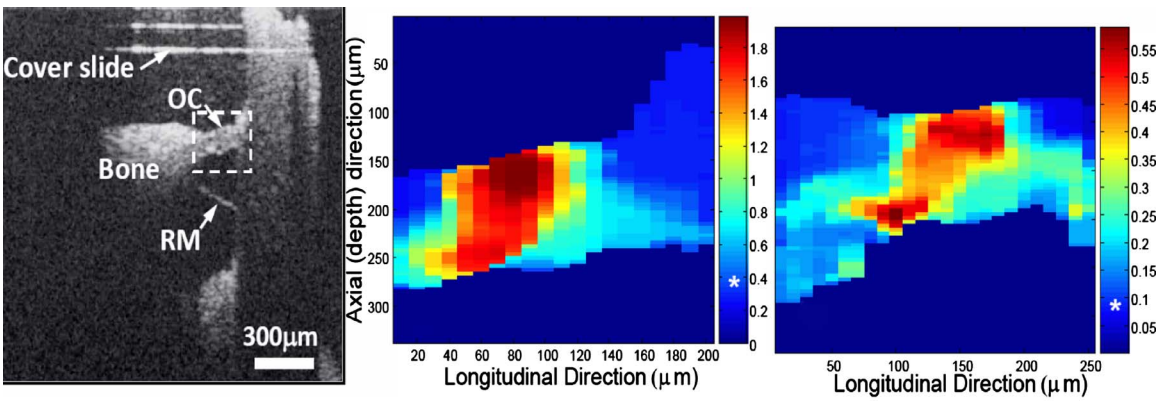

Fig. 6 (A) Cross-sectional image of the OC as imaged by PSOCT system; (B) the corresponding quantitative map of vibrating magnitude for the cross section as marked by the dashed square in (A), with the vibrating source at frequency of 14 KHZ and a magnitude of 0.4 nm; and (C) the same as in (B), but with a frequency of 20 KHZ and a magnitude of 0.1 nm. The color bar at the left of (B) and (C) has a unit of nanometers. The star in the color bar indicates the measured vibrating magnitude from the coverslip. (Color online only.)

our current system resolution ($\sim 16\ \mu$m) is still not high enough to image the cellular morphologies within the OC. An ultra-high-resolution OCT system that uses state-of-the art, broad-bandwidth optical sources, such as a femtosecond laser or a supercontinuum laser, in conjunction with a high-numerical-aperture microscopic objective may, in future development, provide sufficient cellular-level resolution to image the hair cells in the OC.

4 Conclusion

The lack of a high-resolution, highly sensitive, and noninvasive method for imaging the subnanometric tissue motion of the cellular structures within the OC limits our understanding of cochlear biomechanics on how a sound wave propagates through the ribbon-shaped BM, and how the movement of the membrane imparts movement to the cellular and acellular components of the OC, which are attached to the BM. We proposed to use PSOCT to measure the cellular structure motions within the OC at a subnanometer scale and demonstrated its feasibility. We achieved this by measuring the phase changes within the spectral interferograms, imparted by localized tissue motion, and subsequently followed by the FT analyzes. We showed that the conventional SDOCT setup has sufficient sensitivity to measure the depth-resolved vibration with a magnitude as small as 0.05 nm.

Acknowledgments

The authors would like to thank Niloy Choudhury, PhD, and Fangyi Chen, PhD, for assisting in the piezovibration measurements using a laser vibrometer. This work was supported in part by research grants from the National Institute of Deafness and other Communication Disorders (Grants R01DC010399, R01DC010201, and R01DC00141). The content is solely the responsibility of the authors and does not necessarily represent the official views of grant-giving bodies.

References

1. N. P. Cooper and J. J. Guinan Jr., "Efferent-mediated control of basilar membrane motion," *J. Physiol.* **576**(Pt 1), 49–54 (2006).
2. J. Zheng, W. Shen, D. Z. He, K. B. Long, L. D. Madison, and P. Dallos, "Prestin is the motor protein of cochlear outer hair cells," *Nature* **405**, 149–155 (2000).
3. J. Howard, W. M. Roberts, and A. J. Hudspeth, "Mechanoelectrical transduction by hair cells," *Annu. Rev. Biophys. Biophys. Chem.* **17**, 99–124 (1988).
4. P. Martin and A. J. Hudspeth, "Active hair-bundle movements can amplify a hair cell's response to oscillatory mechanical stimuli," *Proc. Natl. Acad. Sci. U.S.A.* **96**, 14306–14311 (1999).
5. D. O. Kim, S. T. Neely, C. E. Molnar, and J. W. Matthews, "An active cochlear model with negative damping in the partition: comparison with Rhode's ante- and post-mortem observation," in *Psychophysical, Physiological Behavioral Studies in Hearing*, G. V. D. Brink and F. A. Bilsen, (Eds.), pp. 7–14, Delft University Press, Delft (1980).
6. W. E. Brownell, C. R. Bader, D. Bertrand, and Y. D. Ribaupierre, "Evoked mechanical responses of isolated cochlear hair cells," *Science* **227**, 194–196 (1985).
7. S. M. Khanna, J. F. Willemin, and M. Ulfendahl, "Measurement of optical reflectivity in cells of the inner ear," *Acta Oto-Laryngol., Suppl.* **467**, 69–75 (1989).
8. S. M. Khanna and L. F. Hao, "Reticular lamina vibrations in the apical turn of a living guinea pig cochlea," *Hear. Res.* **132**, 15–33 (1999).
9. A. W. Gummer, W. Hemmert, and H. P. Zenner, "Resonant tectorial membrane motion in the inner ear: its crucial role in frequency tuning," *Proc. Natl. Acad. Sci. U.S.A.* **93**, 8727–8732 (1996).
10. N. P. Cooper, "An improved heterodyne laser interferometer for use in studies of cochlear mechanics," *J. Neurosci. Methods* **88**, 93–102 (1999).
11. N. P. Cooper, "Vibration of beads placed on the basilar membrane in the basal turn of the cochlea," *J. Acoust. Soc. Am.* **106**, L59–L64 (1999).
12. A. F. Fercher, W. Drexler, C. K. Hitzenberger, and T. Lasser, "Optical coherence tomography—principles and applications," *Rep. Prog. Phys.* **66**, 239–303 (2003).
13. P. H. Tomlins and R. K. Wang, "Theory, development, and applications of optical coherence tomography," *J. Phys. D* **38**, 2519–2535 (2005).
14. G. Hausler and M. W. Lindner, "Coherence radar and spectral radar—new tools for dermatological diagnosis," *J. Biomed. Opt.* **3**, 21–31 (1998).
15. D. Huang, E. Swanson, C. Lin, J. Schuman, W. Stinson, W. Chang, M. Hee, T. Flotte, K. Gregory, C. Puliafito, and J. Fujimoto, "Optical coherence tomography," *Science* **254**, 1178–1181 (1991).
16. W. Drexler and J. G. Fujimoto, "Ultrahigh-resolution ophthalmic optical coherence tomography," *Nat. Med.* **7**(4), 502–507 (2001).
17. J. G. Fujimoto, M. E. Brezinski, G. J. Tearney, S. A. Boppart, B. Bouma, M. R. Hee, J. F. Southern, and E. A. Swanson, "Optical biopsy and imaging using optical coherence tomography," *Nat. Med.* **1**, 970–972 (1995).
18. M. C. Pierce, J. Strasswimmer, and B. H. Park, "Advances in optical coherence tomography imaging for dermatology," *J. Invest. Dermatol.* **123**, 458–463 (2004).
19. B. J. Wong, J. F. de Boer, B. H. Park, Z. Chen, and J. S. Nelson, "Optical coherence tomography of the rat cochlea," *J. Biomed. Opt.* **5**, 367–370 (2000).
20. B. J. F. Wong, Y. Zhao, M. Yamaguchi, N. Nassif, Z. Chen, and J. F. De Boer, "Imaging the internal structure of the rat cochlea using optical coherence tomography at 0.827 μm and 1.3 μm," *Otolaryngol.-Head Neck Surg.* **130**, 334–338 (2004).
21. N. Choudhury, F. Chen, S. K. Matthews, T. Tschinkel, J. Zheng, S. Jackques, and A. L. Nuttall, "Low coherence interferometry of cochlear partition," *Hear. Res.* **220**, 1–9 (2006).
22. H. M. Subhash, V. D. Bhatia, H. Sun, A. T. Nguyen-Huynh, A. L. Nuttall, and R. K. Wang, "Volumetric in vivo imaging of intracochlear microstructures in mice by high-speed spectral domain optical coherence tomography," *J. Biomed. Opt.* **15**, 036024 (2010).
23. S. S. Hong and D. M. Freeman, "Doppler optical coherence microscopy for studies of cochlear mechanics," *J. Biomed. Opt.* **11**, 054014-5 (2006).
24. Z. Chen, Y. Zhao, S. M. Srinivas, J. S. Nelson, N. Prakash, and R. D. Frosting, "Optical Doppler tomography," *IEEE J. Sel. Top. Quantum Electron.* **5**, 1134–1142 (1999).
25. R. K. Wang, Z. Ma, and S. J. Kirkpatrick, "Tissue Doppler optical coherence elastography for real time strain rate and strain mapping of soft tissue," *Appl. Phys. Lett.* **89**, 144103 (2006).
26. R. K. Wang, S. J. Kirkpatrick, and M. Hinds, "Phase sensitive optical coherence elastography for mapping tissue micro-strains in real time," *Appl. Phys. Lett.* **90**, 164105 (2007).
27. F. Chen, N. Choudhury, J. Zheng, S. K. Matthews, A. L. Nuttall, and S. L. Jacques, "In vivo imaging and low-coherence interferometry of organ of Corti vibration," *J. Biomed. Opt.* **12**, 021006 (2007).
28. B. Cense, N. Nassif, T. Chen, M. Pierce, S.-H. Yun, B. Park, B. Bouma, G. Tearney, and J. de Boer, "Utlrahigh-resolution high-speed retinal imaging using spectral-domain optical coherence tomography," *Opt. Express* **12**, 2429–2434 (2004).
29. M. A. Choma, A. K. Ellerbee, C. Yang, T. L. Creazzo, and J. A. Izatt, "Spectral-domain phase microscopy," *Opt. Lett.* **30**, 1162–1164 (2005).
30. C. Joo, T. Akkin, B. Cense, B. H. Park, and J. F. De Boer, "Spectral-domain optical coherence phase microscopy for quantitative phase-contrast imaging," *Opt. Lett.* **30**, 2131–2133 (2005).
31. M. V. Sarunic, S. Weinberg, and J. A. Izatt, "Full-field swept-source phase microscopy," *Opt. Lett.* **31**, 1462–1464 (2006).
32. D. C. Adler, R. Huber, and J. G. Fujimoto, "Phase-sensitive optical coherence tomography at up to 370,000 lines per second using buffered Fourier domain mode-locked lasers," *Opt. Lett.* **32**, 626–628 (2007).

33. C. Joo, K. H. Kim, and J. F. De Boer, "Spectral-domain optical coherence phase and multiphoton microscopy," *Opt. Lett.* **32**, 623–625 (2007).
34. M. C. Skala, M. J. Crow, A. Wax, and J. A. Izatt, "Photothermal optical coherence tomography of epidermal growth factor receptor in live cells using immunotargeted gold nanospheres," *Nano Lett.* **8**, 3461–3467 (2008).
35. D. C. Adler, S. W. Huang, R. Huber, and J. G. Fujimoto, "Photothermal detection of gold nanoparticles using phase-sensitive optical coherence tomography," *Opt. Express* **16**(7), 4376–4393 (2008).
36. R. K. Wang, S. Jacques, S. Ma, S. Hurst, and S. Hanson, "Three dimensional optical angiography," *Opt. Express* **15**, 4083–4097 (2007).
37. R. K. Wang, "In vivo full range complex Fourier domain optical coherence tomography," *Appl. Phys. Lett.* **90**, 054103 (2007).
38. R. K. Wang and L. An, "Doppler optical micro-angiography for volumetric imaging of vascular perfusion in vivo," *Opt. Express* **17**, 8926–8940 (2009).
39. A. Fridberger and J. B. de Monvel, "Sound-induced differential motion within the hearing organ," *Nat. Neurosci.* **6**, 446–448 (2003).
40. A. N. Lukashkin and I. J. Russell, "A second, low-frequency mode of vibration in the intact mammalian cochlea," *J. Acoust. Soc. Am.* **113**, 1544–1550 (2003).